POLITECNICO
MILANO 1863

SCUOLA DI INGEGNERIA INDUSTRIALE
E DELL'INFORMAZIONE

Executive Summary of the Thesis

Modeling of plasma facing component thermal response to runaway electron impact

Laurea Magistrale in Nuclear Engineering - Ingegneria Nucleare

Author: Tommaso Rizzi

Advisor: Prof. Alessandro Maffini (PoliMi)

Co-advisors: Prof. Svetlana Ratynskaia (KTH) , Dr. Panagiotis Tolias (KTH)

Academic year: 2022-2023

1. Introduction and motivation

Several technological and engineering challenges lie on the path to clean renewable energy production by nuclear fusion. The ongoing realization of the ITER project represents a key step in the development of the tokamak magnetic confinement concept and a unique chance to collect invaluable experimental data, getting closer and closer to a commercially feasible energy supply through fusion reactions. Among all challenges to be faced during the operation of such a machine, runaway electrons (REs) are considered of highest priority by the fusion community due to their intense interaction with vessel materials.
In general, the provision of plasma facing components (PFCs) with sufficient lifetime represents one of the major obstacles to overcome in the development of magnetic confinement fusion reactors [7]. Even under normal operating conditions, the PFCs are required to sustain high plasma particle fluxes, continuous neutron irradiation and intense plasma heat loads. Nevertheless, life-time expectations are mostly threatened in the course of transient events such as edge-localized modes (ELMs), major disruptions (MDs) or vertical displacement events (VDEs). The distinguishing characteristic of REs (compared to ELMs, MDs and VDEs) emerges from the fact that electrons with relativistic energies far into the MeV range have depth ranges of the order of millimetres even in high-Z metals like tungsten (W). Thus, RE heat deposition is not only localized but also volumetric in nature. Deep RE-induced melting should severely affect PFC lifetime, whereas RE penetration down to the coolant channels could lead to pipe overpressurization and ultimately to loss-of-coolant accidents with disastrous consequences [2].
Examples of RE-induced damage are illustrated in Fig.1 which features the post-mortem analysis from the PFCs of two different tokamaks, namely JET and FTU. Naturally, RE-induced PFC damage strongly depends on the PFC composition and the RE impact characteristics. In the JET beryllium first wall, RE termination has led to localized melt damage surrounded by radially distributed splash traces [5]. In the FTU molybdenum poloidal limiter, RE impact has led to extensive melt damage and explosive material detachment of solid dust particles ($\sim 50\mu$m) with high speeds around $1\,\mathrm{kms}^{-1}$ [6].
This thesis aims to develop reliable predictive modeling of the complex process of RE-PFC interaction, for which different tools are necessary

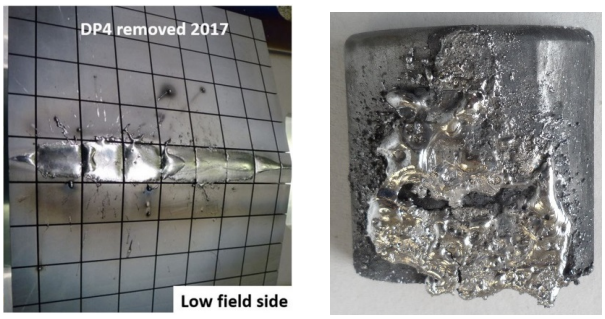

Figure 1: Left: In vessel image of melting on JET tiles removed for post-mortem analysis after ILW-3. Adopted from Ref.[5]. Right: Explosion of FTU poloidal limiter. Adopted from Ref.[6].

(even when the coupled thermo-mechanical PFC response is neglected). First, RE heat deposition into matter has to be modeled through a Monte Carlo (MC) particle transport code. Second, the extracted volumetric heat source has to be incorporated into a heat transfer code to simulate the thermal response including phase transitions. Few attempts have already been carried out along this direction, such as the works by Maddaluno et al [4], Sizyuk & Hassanein [10] or Bazylev et al. [1]. However, existing modeling efforts are typically characterized by oversimplifying assumptions, yet they still serve as a warning for the possible consequences of unmitigated or partially suppressed REs impacting on PFCs. One of the main goal of the thesis concerns the discussion and validation of MC simulations of relativistic RE transport into tokamak relevant materials. For this purpose, the GEANT4 MC-code [9] has been chosen. Benchmarking activities have been carried out to test the accuracy of simulated physics processes among the various options offered by GEANT4. Next, the 3D volumetric heat map outcome of MC runs is incorporated into the MEMENTO melt dynamics code [8] to provide information on the three-dimensional temperature field and the maximum temperature values reached upon RE loading. A fundamental aspect of this project concerns the comparison of the entire workflow with a real case scenario realized in a controlled dedicated experiment. In particular, the modeling predictions have been correlated to the post-mortem analysis of RE-induced damage on graphite PFCs exposed in the DIII-D tokamak.

2. Methodologies and physical processes

As aforementioned, the typical energy range of REs is of the order of MeV. In ITER, the RE beam energies are expected to lie between 1 and 50 MeV. The corresponding depth ranges imply deep electron penetration inside plasma facing components and thus the necessity to consider a volumetric energy deposition when modeling the thermal PFC response. When a relativistic electron penetrates into a solid it leads to the creation of secondary particles like delta electrons, photons or positrons, which also need to be tracked until their thermalization, to collect a complete and precise heat map. Table 1 features the electromagnetic interactions of relevance to RE energy deposition.

INVOLVED EM PROCESSES

Particle	**Process**
Electron e-	Ionisation Scattering Bremsstrahlung
Positrons $e+$	Ionisation Scattering Bremsstrahlung Annihilation
Photons γ	Compton scattering Rayleigh scattering Photo-electric effect Gamma conversion
Excited atoms A^+	Auger transition Radiative transition

Table 1: Particle-matter interactions in the course of electromagnetic showers induced by relativistic electrons in the MeV range.

Particular attention has been paid to the numerical implementation of scattering processes, in dedicated studies of the characteristic trade off between accuracy and computational cost. GEANT4 features 3 possible schemes: *Detailed MC simulations*, where all scattering events (elastic, inelastic) are described in exact chronological succession. *Condensed MC simulations*, where approximate multiple scattering theories are introduced. *Mixed MC simulations*, where the above schemes are appropriately combined.

3. Code validation

A peculiarity of GEANT4 concerns the multiple physics models available for the description of the same particle interaction. Moreover, numerous updates accompany each new version aiming to minimize software bugs and implementation errors. In addition, physics models have specific validity ranges and their accuracy level depends on the energy regime and target composition.
As a result, a systematic validation work is necessary to ensure that the GEANT4 predictions are reliable. The selected benchmark tests comprise calorimetry measurements of the energy deposition profile and collection measurements of the electron backscattering yield. For both quantities, a large number of materials (low-Z, medium-Z, high-Z) has been considered and an extended energy range has been probed. The goal is to build a *Physics List* that contains the most accurate description of electron, positron & photon interactions and that is flexible with respect to the numerical implementation of scattering events (single, mixed, multiple).

3.1. Comparison with calorimetry experiments

High precision experiments were performed at the Sandia National Laboratories [3] featuring nearly mono-energetic electron beams (tens of keV up to 1 MeV), impinging on different materials. The measured quantity is the depth-resolved energy deposition on semi-infinite targets of thickness larger than the electron range and width sufficient to contain the induced electromagnetic shower. The target has been modeled as a cube, whose size complies to the experimental realization. The longitudinal direction has been expressed as a percentage of the CSDA range at the energy of the incident electron beam. The same configuration has been simulated with multiple combinations of physics libraries and scattering implementations.
The basic conclusions from the totality of the simulations are the following. (1) For low Z materials (Be,C), nearly all simulation sets accurately reproduce the experimental data. There are small deviations that are confined to large depths and a small over-shoot of the extended maximum located at approximately half of the CSDA range. Multiple scattering models are nearly indistinguishable from the single scattering implementation. (2) For medium-Z metals (Mo), no simulation is able to reliably reproduce the lowest incident energy results (0.1 and 0.3 MeV). The situation improves as the incident energy increases; at 1.0 MeV all combinations accurately reproduce the experimental data. (3) For high-Z metals (Ta), there are marked differences between the single scattering and multiple scattering implementations that are mainly concentrated near the maximum. The accuracy of single scattering increases with the incident energy, while no multiple scattering schemes are able to reproduce the measurements.

3.2. Comparison with backscattering experiments

Electron backscattering (EBS) refers to the inelastic reflection of incident electrons from the interior of the target back to the ambient. The EBS yield η is defined as the ratio between the total number of backscattered electrons to the number of incident electrons, $\eta = N_{\mathrm{EBS}}/N_{\mathrm{tot}}$. It constitutes an observable that is very sensitive on the numerical implementation of elastic scattering events (single, mixed or multiple). When considering applications to RE termination on PFCs, the materials of interest range from low-Z (such as Be, C) to high-Z metals (such as W). At normal incidence, the primary electron energy has been scanned from 0.1 keV up to 15 MeV. Within the keV range, the electron angle of incidence has been scanned from 0° to 85°. Aiming to understand the sensitivity to the scattering implementation, three sets of simulations have been carried out for each case, combining different scattering models and libraries.
The basic conclusions from the totality of the simulations are as follows. (1) Concerning the sub-keV/keV ranges, G4EmStandardPhysicsSS provides the most satisfactory description of the EBS yield, as highlighted in the representative example of Fig.2. Regardless of the atomic number, it manages to accurately describe the keV energy plateau and it even reproduces the sub-keV monotonic increase in an adequate manner. Moreover, the single scattering model coupled with the PENELOPE library leads to an extended η overshoot for all medium-Z and high-Z materials. Finally, the multiple scattering model coupled with the PENELOPE library yields an erroneous collapse towards zero in the entire sub-

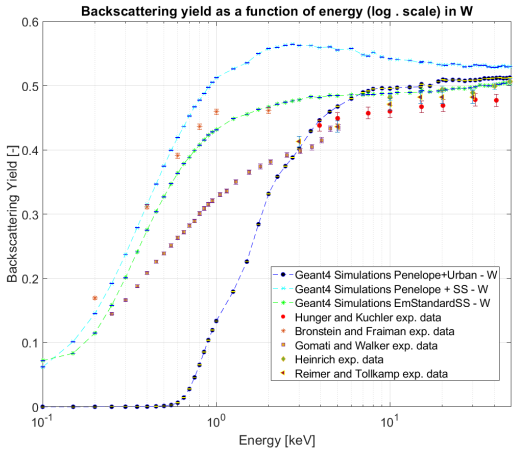

Figure 2: The normal EBS yield of tungsten in the sub-keV and keV energy ranges.

keV range for medium-Z and high-Z materials. Nevertheless, also this simulation set results in a keV energy η plateau close to the experimental one. (2) Concerning the MeV range, it is noted that all three simulation sets reproduce the experimental results with a satisfactory accuracy. (3) Concerning the oblique incidence, given the relatively large probed incident energies (20 keV, 40 keV and 60 keV), again all three simulations sets yield quite accurate results.

4. Modeling of controlled DIII-D experiment

RE-induced damage has been deliberately inflicted on a graphite sample inserted in the DIII-D tokamak with the Divertor Material Evaluation System (DiMES). Experimental input data concerning the sample geometry, magnetic field topology (2.4 T toroidal B-field), wetting configuration, RE energy distribution (mono-energetic at 1 MeV) and RE spatial profile (exponential decay along the vertical) have been included in the GEANT4 simulation. It is worth mentioning that the particle source class has been carefully designed to respect the experimental RE flux and the wetting geometry, while keeping the statistical noise at negligible levels.
GEANT4 simulations have been performed without magnetic field and including the magnetic field only inside the sample. Its effect outside the sample has already been accounted through the empirical impact angles. Specific cross-sections from the 3-dimensional energy deposition maps [J/cm^3] have been plotted in Fig.3 and Fig.4.

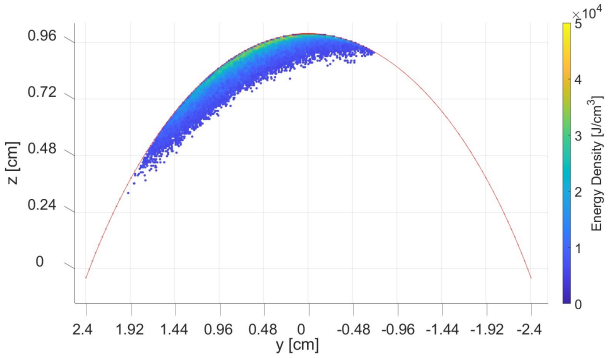

Figure 3: GEANT4 modeling of DIII-D exposure. RE volumetric heat (x = 0 cross section) for $B = 0$ inside the sample.

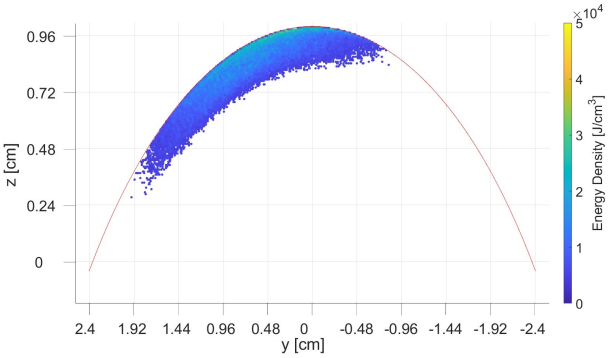

Figure 4: GEANT4 modeling of DIII-D exposure. RE volumetric heat (x = 0 cross section) for $B = 2.4$ T inside the sample.

Without the magnetic field, the energy map is more concentrated in the first layers underneath the surface, with a high peak value represented by the bright yellow color in Fig.3. With the magnetic field inside the sample, a more spread energy deposition pattern emerges, more uniform and peaking at a lower magnitude. Moreover, in spite of the identical energy loading (12.41 kJ), the total amount of energy deposited in this case increases by 11.4%. Particle path tracking demonstrated that, by bending the trajectories due to the gyrating motion along the field lines, the magnetic field reduces the probability that the particles exit the sample domain, thus depositing more energy more uniformly.
The obtained volumetric heat maps have been used as input for the melt dynamic simulation code MEMENTO to compute the thermal response. First, the spherical cap geometry has

been mapped onto a rectilinear grid. In addition, the volumetric heat map has been translated to a power flux by spreading the energy out over 1 ms, which corresponds to the duration of the RE termination event. Naturally, the assessed temperature profiles reflect the volumetric heat source, revealing a lower peak value underneath the surface and a more spread distribution in the non zero field case, see also the 1-D temperature profile presented in Fig.5.

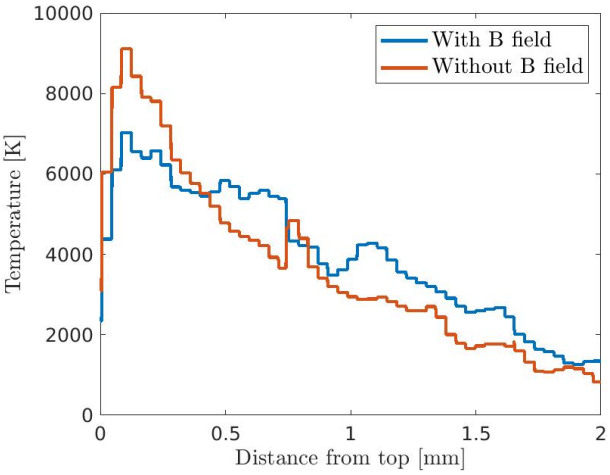

Figure 5: MEMENTO modeling of DIII-D exposure. 1-D temperature profile with and without magnetic field, the x-axis represents a vertical direction starting on top of the dome.

More important, the temperature profiles shed light on the mechanism responsible for material loss during RE impact. With and without magnetic field, the surface temperature is quite modest $\sim$ 3000K, about 900K below graphite's sublimation point. The vapor pressure of graphite at 3000 K is $\sim$ 60 Pa resulting in a negligible erosion rate. A mechanism other than vaporization has to be considered to explain the significant material loss occurring in the experiment. Indeed, the simulated temperature profiles are non-monotonic and peak inside the sample, which implies stress build-up (due to the uneven thermal expansion possibly combined with the large stresses due to internal boiling). This is consistent with the explosive damage mechanism that was observed by the cameras, see also Fig.6 for the correlation between the locus of the temperature maximum and the erosion line.

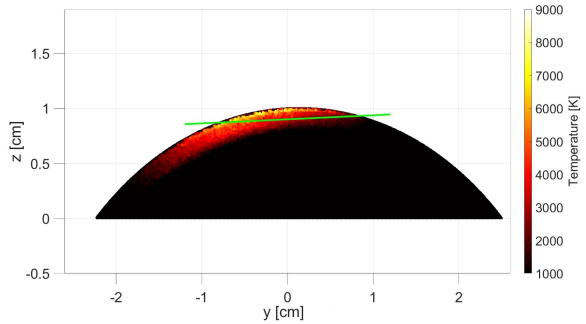

Figure 6: MEMENTO modeling of DIII-D exposure. 2-D temperature profile at the x=0 plane. The green line delimits the material losses as estimated from the post-mortem analysis.

5. Conclusions

Runaway electrons pose a serious threat for the safety of fusion devices. In the course of RE termination, intense heat fluxes are incident on PFCs which can cause extensive damage, as documented in various tokamaks. Characteristic examples concern the localized stationary melting of the Be dump plates in JET and the thermal shock-induced explosion of the poloidal TZM limiters in FTU. This has motivated an intense research on the understanding of RE formation, control and mitigation, particularly in the context of ITER. Despite the remarkable progress concerning RE avoidance, suppression and benign termination, RE-induced damage remains a poorly understood topic. As a consequence, the reliable predictive modeling of the PFC damage triggered by REs is rather imperative.
A major objective in this thesis project is represented by the investigation of relativistic electron transport inside condensed matter, aiming to map the energy deposition inside the material. This constitutes the starting point in the modeling of the complex thermo-mechanical response of the inflicted target, whose complete description would allow the prediction of thermal shock explosions, flying debris characteristics, melt motion and splashing. First, the GEANT4 Monte Carlo code has been selected and a proper validation activity has been carried out against reliable measurements of the longitudinal energy deposition and the electron backscattering yield. This led to the identification of a range of accurate physical models, depending on the target composition and inci-

dent electron energy. In addition, the trade-off between computational cost and accuracy that emerges from the different implementations of scattering events (single, mixed, multiple) has been investigated. Second, GEANT4 has been coupled to the MEMENTO macroscopic melt motion code which can now be employed to model the PFC thermal response to the volumetric RE heat load.
The workflow has been employed for the modeling of the RE-induced damage inflicted on a graphite sample exposed inside the DIII-D tokamak. A non-monotonic temperature profile emerges, reflecting the spatial dependence of the volumetric energy deposition, that is characterized by a modest surface temperature and by a strong peak beneath the surface. The first result allows us to exclude vaporization as the mechanism responsible for the sample erosion, whereas the second result is consistent with the explosive material detachment revealed in the post-mortem analysis. Particular attention is given to the effect of the magnetic field, which alters the charged particle trajectories modifying the energy distribution and even the total amount of energy absorbed.
To complete the development of the GEANT4 simulations, the inclusion of neutron production and related transport processes is envisaged. To optimize the development of the GEANT4 simulations, further benchmarking activities are planned against integrated quantities as well as energy/angle-resolved quantities. Regarding the DIII-D experiment, new simulations are required aiming at a more self consistent approach; the magnetic field will also be included outside the exposed sample and the results of the Kinetic Orbit Runaway electrons Code (KORC) simulations will be utilized to mimic the wetting specifics more faithfully.

References

[1] B. Bazylev et al. Modeling of runaway electron beams for JET and ITER. *J. Nucl. Mater.*, 415:S841–S844, 2011.

[2] F. Maviglia et al. Impact of plasma-wall interaction and exhaust on the EU-DEMO design. *Nucl. Mater. Energy*, 26:100897, 2021.

[3] G. J. Lockwood et al. Calorimetric measurement of electron energy deposition in extended media. Theory vs experiment. 1 1980.

[4] G. Maddaluno et al. Energy deposition and thermal effects of runaway electrons in ITER-FEAT plasma facing components. *J. Nucl. Mater.*, 313-316:651–656, 2003.

[5] I. Jepu et al. Beryllium melting and erosion on the upper dump plates in JET during three ITER-like wall campaigns. *Nucl. Fusion*, 59:086009, 2019.

[6] M. De Angeli et al. Evidence for high-velocity solid dust generation induced by runaway electron impact in FTU. *Nucl. Fusion*, 63:014001, 2022.

[7] R. A. Pitts et al. Physics basis for the first ITER tungsten divertor. *Nucl. Mater. Energy*, 20:100696, 2019.

[8] S. Ratynskaia et al. Experiments and modelling on ASDEX Upgrade and WEST in support of tool development for tokamak reactor armour melting assessments. *Nucl. Mater. Energy*, 33:101303, 2022.

[9] Geant4 community. *Geant4, a simulation toolkit.* Available on line, https://geant4.web.cern.ch/about/.

[10] V. Sizyuk and A. Hassanein. Self-consistent analysis of the effect of runaway electrons on plasma facing components in ITER. *Nucl. Fusion*, 49:095003, 2009.